Enzymatic Synthesis of $^{18}O(6)$-Guanosine and Spectroscopic Characterization of Hoogsteen and Reverse Hoogsteen Hydrogen-Bonded Guanosine Structures

Arantxa Rodríguez-Casado,† Pedro Carmona,*,† and Marina Molina‡

Instituto de Estructura de la Materia (CSIC), Serrano 121, 28006-Madrid, Spain, and Departamento de Química Orgánica I, Escuela Universitaria de Optica, Arcos de Jalón s/n, 28037-Madrid, Spain

Received: February 17, 1998; In Final Form: April 7, 1998

Adenylic acid deaminase has been successfully used for the first time to convert Cl(6)-guanosine to $^{18}O(6)$-guanosine in the presence of $H_2{}^{18}O$. Observations of infrared and Raman spectra of both guanosine and $^{18}O(6)$-guanosine permit assignment of the carbonyl vibrations in guanosine tetramer. In-plane normal mode wavenumbers have been calculated using a valence force field that incorporates an interaction force constant of νC═O transition dipole coupling. This coupling alone between carbonyl groups of adjacent guanine residues provides the physical basis for understanding the observed C═O splittings in guanosine tetramer and in hydrogen-bonded guanine bases adopting the Hoogsteen structure. This coupling is, however, absent in the dimer of 2′-deoxy-3′,5′-bis(triisopropylsilyl)guanosine, which is known to adopt the reverse Hoogsteen structure. The νC═O spectral profiles, then, permit the distinction between Hoogsteen and reverse Hoogsteen hydrogen-bonded guanine nucleobases in G*G·C triplets that may be present in nucleic acid triple helices.

1. Introduction

A considerable number of studies have been reported concerning the vibrational spectra of nucleic acids and of guanosine in particular.[1−5] However, some aspects of the vibrational spectra of hydrogen-bonded guanosine forming part in guanosine-guanosine-cytidine (G*G·C) triplets and in poly-(G) quadruple helices have not yet been undertaken. Two different hydrogen-bonding schemes have been suggested between two guanines, corresponding respectively to the so-called Hoogsteen and reverse Hoogsteen hydrogen bonding (Figure 1) by analogy with the model proposed by Hoogsteen for hydrogen bonding between adenine and thymine. These hydrogen-bonded structures, nevertheless, have not yet been satisfactorily characterized using vibrational spectroscopy. What remains to be understood is that guanine in G*G·C trimers of some dG_n*dG_n·dC_n triple helices, to which a hydrogen-bonded Hoogsteen structure has been attributed on the basis of molecular mechanics calculations,[6−8] generates two νC═O strong bands in the infrared spectrum. This contrasts with the unique νC═O band of the reverse Hoogsteen hydrogen-bonded guanine, as shown in this work. The higher frequency νC═O band component of the above triple helices appearing near 1715 cm^{-1} has been tentatively assigned to the unbound C═O stretching vibration of the Hoogsteen G*G·C triplets.[6] However, this cannot be the ultimate cause of the appearance of two guanine νC═O bands from these triplets, as one guanine carbonyl group is also unbound in the reverse Hoogsteen structure of G*G dimer and G*G·C trimer (Figure 1).

One possible strategy is the recording of the spectra of hydrogen-bonded substances that are known to adopt the above structures, as determined by X-ray crystallography or other techniques, and assigning the spectral features by use of isotopic derivatives and theoretical calculations with an appropriate force field. Up to now, no crystallographic study dealing with structure of dG_n*dG_n·dC_n triple helices has been carried out. However, guanosine itself in aqueous solution cooled to 10 °C forms gels having tetrameric species with the Hoogsteen hydrogen-bonded guanosine structure.[9] On the other hand, it was proved that a different hydrogen-bonded molecular species having the guanosine reverse Hoogsteen structure is the G*G dimer formed in solutions of 2′-deoxy-3′,5′-bis(triisopropylsilyl)-guanosine.[10] The force fields of two adjacent guanine nucleobases in these hydrogen-bonded nucleosides may include some particular force constants generating the respective spectral profiles that are characteristic of the above structures.

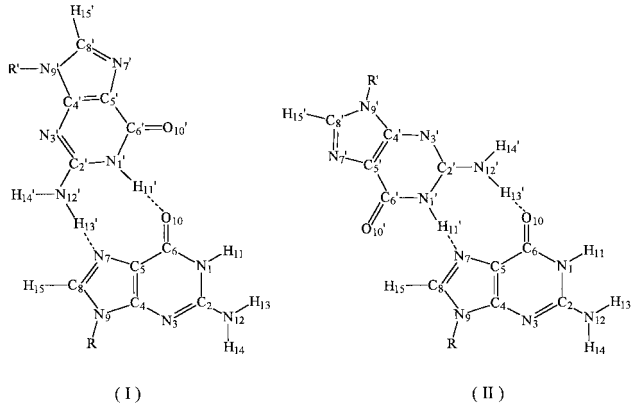

Figure 1. Hoogsteen (form I) and reverse Hoogsteen (form II) hydrogen-bond patterns of G*G dimer.

With this aim, we have prepared tetrameric species of guanosine and $^{18}O(6)$-guanosine as well as dimeric species of the above silanized guanosine and report here the analysis of their vibrational spectra on the basis of isotopic frequency shifts and normal mode calculations. Transition dipole coupling is seen to provide a consistent explanation for the characteristic νC═O splittings in tetrameric guanosine and in other hydrogen-

* To whom correspondence should be addressed: Fax +34 91 5645557; E-mail pcarmona@pinar1.csic.es.
† Instituto de Estructura de la Materia.
‡ Escuela Universitaria de Optica.

S1089-5647(98)01189-4 CCC: $15.00
Published on Web 06/11/1998

TABLE 1: Enzyme-Catalyzed Preparative Synthesis of ^{18}O(6)-Guanosine

reaction[a]	substrate (mg)	enzyme (mg)	pH	T (°C)	reaction time (days)	yield (%)
1	10	20	<5.0	25	7	<25
2	10	20	6.2	25	7	100
3	10	20	6.2	38	5	100
4	40	20	6.2	38	6	100
5	40	20	6.2	38	5	100
6	30	50	6.2	38	4	100

[a] Crude and purified enzyme preparations were used in the 1−4 and 5−6 reactions, respectively.

bonded guanine species where two adjacent guanine bases adopt the Hoogsteen structure.

2. Experimental Section

2.1. Materials. 6-Chloroguanosine, supplied by Sigma with purity greater than 95%, was used without further purification. 5′-Adenylic acid deaminase (AMPDA) from *Aspergillus* species was also purchased from Sigma (0.1 unit/mg of solid). This enzyme was purchased as a lyophilized powder containing approximately 20% protein, with the balance being primarily diatomaceous earth. To purify the protein, the crude enzyme was suspended in water, the solid residue was filtered off, and the aqueous solution of the enzyme was dried under vaccum to obtain the solid protein used in the enzymatic reactions. $H_2{}^{18}O$ was obtained from CIL (Cambridge Isotope Laboratories) with isotopic purity greater than 98%.

2′-Deoxy-3′,5′-bis(triisopropylsilyl)guanosine and 2′-deoxy-3′,5′-bis(triisopropylsilyl)cytidine, which will be referred to as G and C, respectively, were prepared as described elsewhere.[10] The N-deuterated isotopic derivatives of these silanized nucleosides were obtained by repeated exchanges of chloroform solutions of these substances with C_2H_5OD until the elimination of the infrared NH stretching absorption was achieved.

2.2. Enzymatic Synthesis of ^{18}O(6)-Guanosine. This isotopic derivative of guanosine was obtained from Cl(6)-guanosine as follows (Table 1). To 1 mL of $H_2{}^{18}O$ buffer solution (0.08 M cacodylate, pH 6.20) containing 20−50 mg of enzyme was added 10−40 mg of Cl(6)-guanosine. The suspension was incubated at 25−38 °C for the periods of time indicated in Table 1 and the reaction mixture was examined through thin-layer chromatography. Complete solution of Cl-(6)-guanosine occurred after 2−3 h from the start of the enzyme reaction. ^{18}O(6)-Guanosine precipitated from solution within the first day of the reaction. After the complete conversion of the starting substrate to the above guanosine isotopic derivative, the enzyme was filtered off and the guanosine precipitate was purified by chromatography on Sephadex G-25 medium, with water as an eluent. The resulting guanosine solution was lyophilized to obtain ^{18}O(6)-guanosine in a powdery form. This isotopic derivative was then characterized by infrared spectroscopy and mass spectrometry and elemental analysis.

N-Deuterated guanosine was prepared by repeated exchanges with hot heavy water and checking the absence of NH and OH stretching bands in the infrared spectra of solid films.

Guanosine gels were prepared by heating at 100 °C aqueous solutions containing 0.03 M guanosine and 0.1 M KCl, to dissolve this nucleoside. The heated solutions were then cooled at 10 °C, which led to the formation of guanosine viscous gels.

2.3. Spectroscopy. Fourier transform infrared (FTIR) spectra were recorded on a Perkin-Elmer 1725X spectrophotometer coupled to a personal computer. Usually 65 scans were performed, and the data transferred to the computer were treated with Perkin-Elmer software. This treatment included multiple baseline corrections and smoothing by the Savitsky and Golay procedure.

Usual infrared cells of thickness ranging from 0.1 mm to 1 cm were used to record the infrared spectra of guanosine gels and the ditriisopropylsilylated nucleosides in chloroform solution. The infrared cells used for the study of guanosine films are of the same kind as those described in other work.[11] Film specimens of guanosine in the solid state were cast from aqueous solution and deposited on a ZnSe window. The specimens were then sealed in a homemade sample holder allowing exposure of the film to the desired humidities.

Raman spectra were run at 3 cm^{-1} resolution using a Jobin-Yvon Ramanor U-1000 spectrometer equipped with double monochromator, two holographic gratings, and a single-channel PM detector. The 514.5 nm line of a Spectra Physics 165 argon ion laser was used for excitation (power at the source 400 mW), and the spectra were obtained from the average of at least 10 scans.

2.4. Computational Details. The GF technique of Wilson[12] was applied to hydrogen-bonded guanosine tetramer and dimer adopting the Hoogsteen and reverse Hoogsteen structures. The structural parameters were taken from X-ray data,[13,14] and the guanine base was considered to be planar. For the sake of simplicity only the bases have been shown in the figures of guanosine tetramer and dimers. The additional sugar is located at the site denoted by R (ribose). This was done since our main aim here has been to emphasize the fairly localized νC═O stretching region of N-deuterated guanosine, and this region is not influenced by the ribose residue. Thus, we have assumed the absence of any vibrational interaction between ribose and the C═O groups and, hence, carried out the normal coordinate calculations by considering only the hydrogen-bonded guanine bases. The internal coordinates, along with the force constants for guanine and hydrogen bonds, were transferred from previous works.[15−17] To respect the harmonic potential approximation, the redundant internal coordinates have been removed by following literature methods.[15,16] Effects due to transition dipole−dipole coupling interactions of the C═O dipoles were incorporated as described by Moore and Krimm.[18]

3. Results and Discussion

3.1. Enzymatic synthesis of ^{18}O(6)-Guanosine. The results from the synthesis of this isotopic derivative of guanosine are included in Table 1.

Six different reactions were carried out to achieve the optimum enzyme activity. In this respect, the pH was found to be the most crucial condition to achieve the completion of the enzymatic reaction. This can be explained by assuming that the native conformational structure and, hence, the enzymatic activity of the protein is lost to some extent in acidic medium. pH was, hence, controlled carefully throughout the whole synthesis by using buffered reaction mixtures.

It has been suggested that dechlorination of purines may involve addition of a water molecule and elimination of Cl$^-$ or a nucleophilic S_N2 mechanism by which a water hydroxyl group acts as nucleophilic reagent.[19] In any case, quantitative formation of guanosine is expected due to the fact that the reaction is irreversible (Figures 2 and 3). As guanosine is slightly soluble in water, the course of the reaction can be observed quantitatively by recording the infrared spectra of the solution in which the reaction was carried out. By comparison of the normalized spectra (Figure 2), it is noted that the carbonyl 1664 cm^{-1} band of guanosine increases as the reaction proceeds, and the same

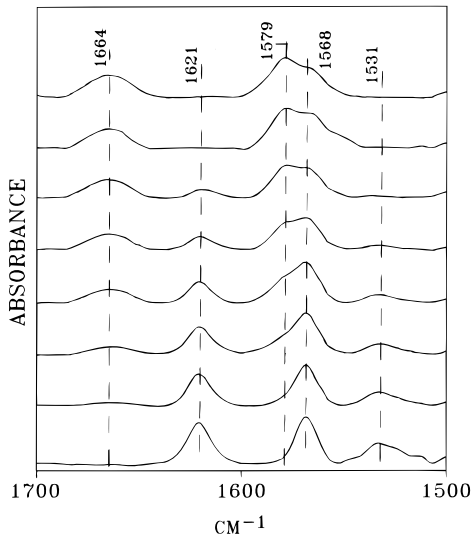

Figure 2. Enzymatic conversion of Cl(6)-guanosine to guanosine in D_2O followed through infrared spectroscopy: (from top to bottom) 4 days, 3 days, 2 days, 1 day, 12 h, 6 h, 3 h, and 0 h. The same reaction course was observed for ^{18}O(6)-guanosine synthesis.

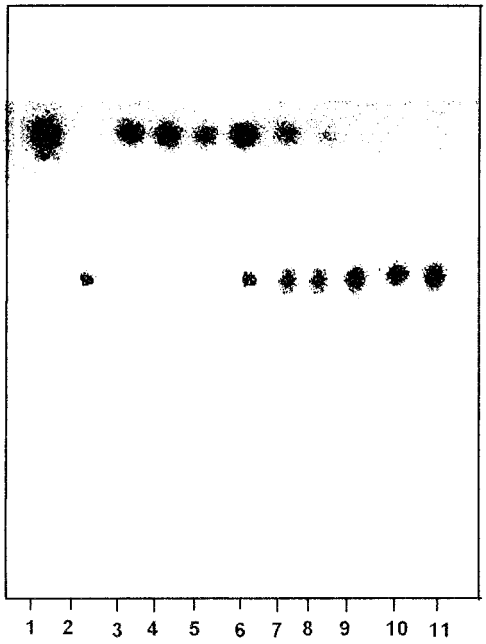

Figure 3. Enzymatic conversion of Cl(6)-guanosine to ^{18}O(6)-guanosine followed through thin-layer chromatography. Tracks 1 and 2, Cl(6)-guanosine and ^{18}O(6)-guanosine, respectively. Tracks 3−11, reaction times ranging from 0 to 4 days: time 0, 30 min, 1 h, 3 h, 12 h, 1 day, 2 days, 3 days, and 4 days.

can be said for the 1579 cm^{-1} band characteristic of this nucleoside. These spectral changes are accompanied by decreasing intensities of the 1621 and 1531 cm^{-1} bands corresponding to Cl(6)-guanosine. Moreover, the reaction course is, obviously, the same for both guanosine and ^{18}O(6)-guanosine, is clean, and proceeds without formation of byproducts. On the other hand, the reaction can be run either at room temperature or at 38 °C to increase the reaction rates (Table 1). The results also show that the purified enzyme is as active as the crude one. Production of molecules labeled with stable isotopes is, then, attractive because the yield of enzymatic methods is practically 100% when irreversibility of the reaction can be achieved through elimination of one of the end products. This is the case of the above reaction, where guanosine is eliminated through precipitation due to the fact that this

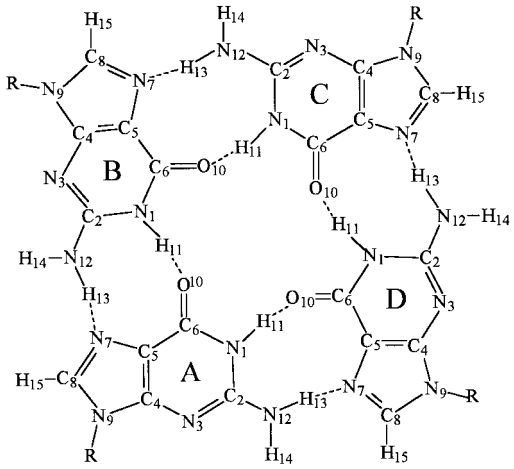

Figure 4. Schematic representation of centrosymmetric hydrogen-bonded guanosine tetramer.

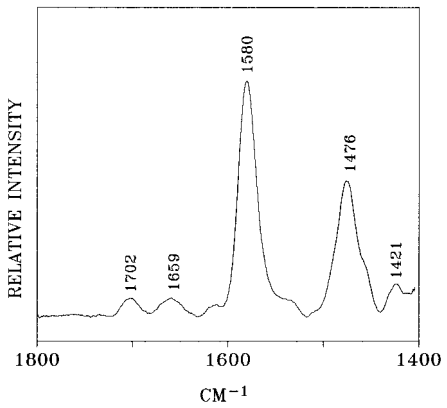

Figure 5. Raman spectrum of a gel of guanosine (0.03 M) in D_2O + KCl (0.1 M) at 10 °C.

compound is not soluble at the pH used. This enzyme was also used in a previous work[20] for quantitative deamination or demethoxylation of a variety of purine ribosides. As it has been shown that this enzyme has a very broad substrate specificity, we have used it for the first time for the synthesis of ^{18}O(6)-guanosine by dechlorination of Cl(6)-guanosine. The enzyme and substrate are inexpensive and available commercially and can be used for large-scale synthesis of this guanosine isotopic derivative.

3.2. Spectra and Assignments. Guanosine and its analogues are known to form gels in concentrated aqueous electrolytic solutions[21,22] and there is evidence[23−26] that supports the tetrameric arrangement between guanosine residues proposed by Gellert et al.[22] These centrosymmetric tetrameric species (Figure 4) are assumed to be planar (C_{2h} symmetry). Thus, four in-plane νC═O vibrational modes can be expected from this hydrogen-bonded molecular species, two of which are Raman-active (A_g symmetry) and two of which are infrared-active (B_u symmetry).

The Raman and infrared spectra of N-deuterated guanosine gels are presented in Figures 5 and 6. The Raman spectrum shows two weak bands at 1702 and 1659 cm^{-1} that are attributable to C═O stretching motions. These two bands are replaced by another band at 1671 cm^{-1} that emerges upon melting of the guanosine gel.[1] The 1702 and 1659 cm^{-1} Raman bands are, hence, produced by hydrogen-bonded carbonyl groups in guanosine tetrameric species. In heavy water, the NH_2 and NH groups of guanine should be deuterated and no NH_2 and NH in-plane bending vibrations are expected in the 1700−1400

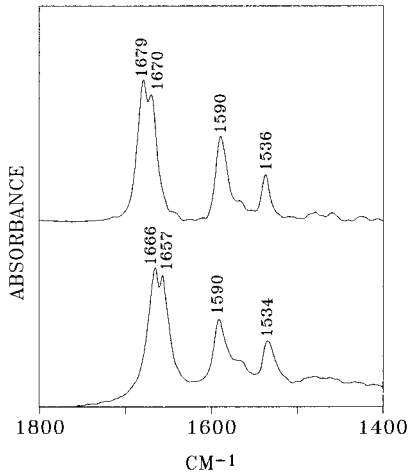

Figure 6. Infrared spectra of gels of guanosine (0.03 M) in D_2O + KCl (0.1 M) at 10 °C: (upper) guanosine and (lower) $^{18}O(6)$-guanosine.

cm^{-1} region. All the other nucleobase bands observed in this region are, hence, attributed to ring vibrations, the strong ones located at 1580 and 1476 cm^{-1} being of pyrimidic and imidazolic character respectively.[1,15,16] The strong band near 1580 cm^{-1} is observed in all the spectra of compounds containing the guanine residue. The observed ^{15}N shifts for guanosine and its N-deuterated analogues are 7 cm^{-1} for the pyrimidic substitution instead of 0−2 cm^{-1} for the imidazolic labeling.[1] The band near 1480 cm^{-1} is characterized by a large frequency shift of 23 cm^{-1} upon the C_8−H deuteration in guanosine,[27] and this was used as a monitor band of the C_8−H deuterium exchange kinetics.[27] This band also shows a marked frequency shift and/or intensity change on the coordination at N^7 of heavy metal ions and on N^7 protonation.[28−30]

The infrared spectrum of guanosine gel in heavy water (Figure 6) shows two strong bands at 1679 and 1670 cm^{-1}, which shift to 1666 and 1657 cm^{-1} upon ^{18}O isotopic labeling of the nucleobase carbonyl group. The strong relative intensities of these bands and their frequency shifts upon ^{18}O isotopic substitution support their assignment to the stretchings of C═O groups. As described for the Raman spectrum, the other normal modes generated by the nucleobase in the 1700−1400 cm^{-1} infrared region correspond to ring vibrations, with the most prominent bands occurring at 1590 and 1536 cm^{-1}. A ^{15}N shift of about 17 cm^{-1} has been observed in deuterated DNA and the totally ^{15}N substituted analogue for the infrared band near 1590 cm^{-1} attributed mainly to the pyrimidic ring of guanine residue,[31] and the infrared band observed near 1535 cm^{-1} is associated with a mode involving imidazolic and pyrimidic ring stretching motions.[1,16]

The characters of the nucleobase vibrational modes in the 1800−1500 cm^{-1} region do not depend on whether guanine is linked with ribose, as sugar groups do not contribute in this region.[32] For instance, the Raman bands observed for guanosine are very similar to those observed for 9-ethylguanine.[32] Our main aim here has been, hence, to restrict ourselves to this region, which includes the fairly localized C═O stretching modes, as described above. As these groups take part in the hydrogen bonds of the guanosine nucleobases, the νC═O bands can give information on the structures of hydrogen-bonded guanine residues.

3.3. Intermolecular Interaction Effects in the νC═O Vibrations. In reference to the νC═O infrared and Raman bands, a question arises as to the physical mechanism that accounts for the above νC═O splittings. In this respect, there seems to be some coupling between the νC═O vibrations, as

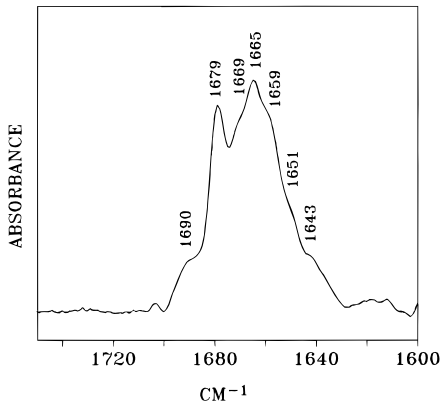

Figure 7. Infrared spectrum of a isotopically mixed gel [guanosine/$^{18}O(6)$-guanosine 1/1 mol ratio] in D_2O containing 0.03 M guanosine and 0.1 M KCl at 10 °C.

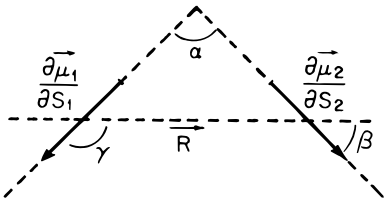

Figure 8. Interacting transition dipoles.

reflected by the fact that the νC═O frequencies in the infrared and Raman spectra are not coincident. This coupling is also supported by the infrared spectrum of a gel containing guanosine and $^{18}O(6)$-guanosine in a 1/1 mol ratio (Figure 7). In fact, gels prepared by mixing equimolar aqueous solutions of both guanosine isotopic derivatives obviously produce various tetrameric hydrogen-bonded molecular species having C_s and C_{2h} symmetries, depending on the positions of the labeled guanosine molecules in each tetrameric molecule. If the stretching motions of carbonyl groups are coupled, there should be more νC═O bands in the infrared spectrum of the isotopically mixed gel in comparison with the infrared spectra of the pure isotopic derivatives (Figure 6), as all of the νC═O vibrations of C_s tetramers are infrared-active. Figure 7 shows that this is the true situation and the carbonyl stretching motions, hence, are coupled.

Accordingly, the intramolecular valence force field[15,16] and hydrogen-bonding force constants[17] are not sufficient to reproduce the observed νC═O frequencies, and it is necessary to incorporate interaction force constants between the carbonyl group stretchings. Transition dipole coupling provides a reasonable physical basis for these interactions, as described below and shown in Figure 8.

The potential energy between two transition dipoles originated with respect to each other[17,18] is given by

$$V = \frac{1}{\epsilon}\frac{|\delta\mu_1/\delta S_1||\delta\mu_2/\delta S_2|}{|R|^3}(\cos\alpha - 3\cos\beta\cos\gamma)S_1S_2 \quad (1)$$

where ϵ is the dielectric constant (taken here to be 1), $\delta\mu_i/\delta S_i$ is a transition dipole moment, and S_i is a stretching coordinate (V is in ergs for quantities in cgs units). If both transition dipoles are associated with νC═O motions in both hydrogen-bonded nucleobases, the interaction force constant between the two transition dipoles is, therefore, in millidynes per angstrom

$$f = 0.1(\delta\mu/\delta r_{C=O})^2 X \quad (2)$$

TABLE 2: Force Constants for In-Plane Modes of Guanine Tetramer

	Diagonal		
N_1C_2	5.5	$C_4C_5C_6$	1.05
C_2N_3	6.54	$C_5C_6N_1$	0.92
N_3C_4	6.48	$C_6N_1C_2$	1.18
C_4C_5	6.3	$C_5N_7C_8$	1.63
C_5C_6	5.9	$N_7C_8N_9$	1.99
N_1C_6	5.79	$C_8N_9C_4$	1.48
C_5N_7	5.64	$C_5C_4N_9$	1.27
N_7C_8	7.55	$C_6C_5N_7$	0.94
C_8N_9	6.25	$C_4C_5N_7$	0.9
C_4N_9	6.2	$N_3C_4N_9$	1.36
C_6O_{10}	9.89	$N_3C_2N_{12}$	1.7
C_2N_{12}	5.5	$N_1C_2N_{12}$	1.72
N_1H	4.71	$C_2N_{12}H$	0.431
N_9H	4.71	$HN_{12}H$	0.222
$N_{12}H_{13}$	5.70	C_2N_1H	0.422
$N_{12}H_{14}$	5.84	C_6N_1H	0.43
C_8H	5.36	$N_1C_6O_{10}$	0.94
O_{10}...H_{11}	*0.15*	$C_5C_6O_{10}$	0.722
N_7...H_{13}	*0.15*	N_7C_8H	0.423
$N_1C_2N_3$	0.96	N_9C_8H	0.398
$C_2N_3C_4$	1.90	C_8N_9H	0.389
$N_3C_4C_5$	1.26	*$N_{12}H_{13}$...N_7*	*0.01*
C_4N_9H	0.388	*C_6O_{10}...H_{11}*	*0.01*
	Interaction Force Constants[a]		
f(ν_r, ν_r) (*ortho*)	0.85	f(C_6O_{10}, δC_6O_{10})	0.5
f(ν_r, ν_r) (*meta*)	0.64	f(C_6O_{10}, ν_r)	0.8
f(ν_r, ν_r) (*para*)	−0.140	f(δC_6O_{10}, ν_r)	0.45
f(ν_r, δ_r)	0.2	f(C_8H, ν_r)	0.41
f(ν_r, NH)	0.2	f(δC_8H, ν_r)	0.28
f(ν_r, δNH)	0.063	f(δNH, NH)	0.094
f(C_4C_5, C_6O_{10})	−0.03	*f(C_6O_{10}, C_6O_{10})*	*0.180*

[a] ν_r refers to ring bond stretching and δ_r to ring interbond angle deformation. Intermolecular force constants are shown in italics, and *f*(C_6O_{10}, C_6O_{10}) refers to the interaction force constant of carbonyl groups in adjacent nucleobases. Stretching and deformation force constants and *f*(ν_r, ν_r) and *f*(ν_r, δ_r) are given in millidynes per angstrom, (millidynes)·(angstroms), millidynes per angstrom, and millidynes, respectively.

where $X = (\cos\alpha - 3\cos\beta\cos\gamma)/R^3$ is the geometrical factor, with R given in angstroms and $\delta\mu/\delta r_{C=O}$ given in Debyes per angstrom $= 10^{-10}$ esu.

If we use the above equations to calculate f from a transition dipole coupling mechanism, then we find that for a C···C distance of 3.87 Å (for adjacent carbonyl groups, Figure 4) and a transition dipole centered at the midpoint of the C═O bond, the interaction force constant is given by $0.0025(\delta\mu/\delta r_{C=O})^2$. Although the transition dipole moment is unknown, values of the order of 9−10 may be reasonable.[18,33] This would give f = 0.20 mdyn/Å (whereas $\delta\mu/\delta r_{C=O} = 10$ would give $f = 0.25$ mdyn/Å).

A f value of 0.20 mdyn/Å as well as the force constants proposed by Majoube[15,16] for the in-plane modes have been introduced as input data in the calculations. The force field has been refined to fit the infrared and Raman frequencies, and the final values of the force constants are reported in Table 2.

An interaction constant, K, is defined as $K = (\delta\nu/\delta f)f$, the total splitting between components being $\Delta\nu = 2K = 2(\delta\nu/\delta f)f$. A normal mode calculation for guanosine tetramer using the force field of Table 2, with and without a *f*(νC═O, νC═O) term, shows that, for the higher frequency Raman band near 1700 cm^{-1}, $K = 24 = 127f$(νC═O, νC═O), whereby *f*(νC═O, νC═O) ≅ 0.18 mdyn/Å. On the other hand, the above values of f obtained with eqs 1 and 2 are approximately 0.18 mdyn/Å. Thus, it seems that the transition dipole coupling mechanism gives the correct sign of *f*(νC═O, νC═O) and a value that is of the appropriate order of magnitude.

The in-plane normal modes calculated through this force field are shown in Table 3 for guanosine tetramer whose infrared and Raman νC═O bands are fairly well reproduced by this calculation. A question that has remained unanswered is why the higher- and lower-wavenumber νC═O bands are not infrared-active. We believe that this may be explained on the basis of transition dipole−dipole coupling arguments, along with knowledge of transition probability in quantum mechanics.[34] Infrared band intensities are related to the expression for transition probability

$$\omega = (2\pi/h)\rho(k)|\langle k|H'|m\rangle|^2$$

where $\rho(k)$ is the density of final states, m is the initial state, and H' is the interaction responsible for the transition. This is a general expression. In the case of infrared bands, H' is the value of the transition dipole moment associated with the given vibration. Although quantitative relative band intensities are too complicated to understand at the present stage, a qualitative prediction could be made on the basis of the eigenvectors involved in a normal mode. A look at Table 4 shows that, for the computed frequencies at 1700 and 1659 cm^{-1}, the values of the eigenvector components of nonadjacent carbonyl groups are very similar and of the same signs. This means that the net change in the dipole moment during these vibrations is going to be nearly zero. When this is so, the expression for the transition probability will have an insignificant value, which means that the corresponding infrared bands are not going to be seen in the spectra.

Our results presented here demonstrate that the adjacent C═O transition dipole moments interact strongly, as a force field without the *f*(νC═O, νC═O) force constant generated from the interaction between carbonyl groups in adjacent nucleobases (Table 2) does not reproduce the νC═O vibrational modes well. Moreover, a good frequency agreement does not involve the use of an additional force constant related to the interaction between the nonadjacent carbonyl groups. This means that coupling between the transition dipoles associated with these C═O stretching vibrations is very weak, maybe due to the great distance between these nonadjacent carbonyl groups. In fact, using eq 2 to calculate *f*(νC═O, νC═O) and taking the 5.48 Å C···C distance from the structure proposed by Davies et al.,[14] we find that for $(\delta\mu/\delta r_{C=O}) = 9$ the value of *f*(νC═O, νC═O) is 0.05. However, incorporation of this force constant into the force field does not provide a significant improvement in the good frequency agreement previously obtained with the use of the alone interaction force constant generated by the adjacent carbonyl groups.

As transition dipole moment depends on the distance between the carbonyl groups and their relative orientations, it is reasonable to assume that the above coupling occurs whenever two adjacent hydrogen-bonded guanine nucleobases adopt the Hoogsteen structure. Thus, if the force field of Table 2 is applied to a Hoogsteen G*G dimer or G*G·C trimer, a νC═O splitting of about 20 cm^{-1} is obtained. Transition dipole coupling must, then, be the origin of the νC═O splitting observed in the vibrational spectra of the dG_n*dG_n·dC_n triple helices[6] to which Hoogsteen structure for the G*G·C triplets was attributed on the basis of molecular mechanics calculations. Moreover, the previous assignment of the two νC═O bands to the hydrogen-bonded and free C═O groups in Hoogsteen structure[6] found in the above dG_n*dG_n·dC_n triple helices is not consistent with the fact that the homodimer of 2′-deoxy-3′,5′-bis(triisopropylsilyl)guanosine, which has been found to adopt the reverse Hoogsteen structure in chloroform solution,[10,35] does

TABLE 3: Observed and Calculated In-Plane Frequencies (cm^{-1}) of Guanine Tetramer[a]

infrared	Raman	calculated	assignments (PED/%)
	1702 w	1700 (19)	νC═O (18_A); νC═O (18_B); νC═O (18_C); νC═O (18_D)
1679 vs (14)		1680 (15)	νC═O (34_A); νC═O (32_C); νC_5C_6 (9_C); νC_5C_6 (7_A)
1670 vs (13)		1673 (14)	νC═O (36_B); νC═O (36_D); νC_5C_6 (8_B); νC_5C_6 (8_D)
	1659 w	1659 (12)	νC═O (16_B); νC═O (16_D); νC═O (14_A); νC═O (13_C); νC_5C_6 (6_A); νC_5C_6 (6_C)
1639 vw (−)		1635 (4)	νC_4C_5 (26_C); νN_3C_4 (12_C); νC═O (11_C); νC_2N_3 (9_C)
		1627 (2)	νC_4C_5 (21_A); νN_3C_4 (14_A); νC_2N_3 (9_A); νC_4C_5 (6_B); νC_4C_5 (5_D)
	1615 vw	1627 (2)	νC_4C_5 (16_B); νC_4C_5 (16_D); νN_3C_4 (11_D); νN_3C_4 (10_B); νC_2N_3 (7_B); νC_2N_3 (7_D)
		1626 (4)	νC_4C_5 (10_A); νC_4C_5 (8_B); νC_4C_5 (5_D); νN_3C_4 (7_A); νN_3C_4 (6_B); νN_3C_4 (6_D)
		1591 (0)	νC_2N_3 (28_C); νN_1C_2 (23_C); $\delta C_2N_3C_4$ (12_C); $\delta N_3C_2N_{12}$ (11_C)
1590 s (0)	1580 vs	1591 (0)	νC_2N_3 (12_A); νN_1C_2 (10_A); νC_2N_3 (8_B); νC_2N_3 (7_D); νN_1C_2 (6_B); νN_1C_2 (6_D); $\delta C_2N_3C_4$ (6_A); $\delta N_3C_2N_{12}$ (5_A)
		1591 (0)	νC_2N_3 (14_D); νC_2N_3 (13_B); νN_1C_2 (11_D); νN_1C_2 (10_B); $\delta C_2N_3C_4$ (6_B); $\delta C_2N_3C_4$ (6_D); $\delta N_3C_2N_{12}$ (6_D); $\delta N_3C_2N_{12}$ (5_B)
		1591 (0)	νC_2N_3 (15_A); νN_1C_2 (12_A); νC_2N_3 (7_B); $\nu\delta C_2N_3C_4$ (7_A); νC_2N_3 (6_D); $\delta N_3C_2N_{12}$ (6_A); νN_1C_2 (5B); νN_1C_2 (5_D)
		1552 (0)	νC_2N_{12} (14_A); νC_2N_{12} (8_B); νC_2N_{12} (8_D); νC_2N_3 (5_A); νC_2N_3 (5_B)
1561 w (0)		1551 (0)	νC_2N_{12} (15_B); νC_2N_{12} (15_D); νC_2N_3 (5_B); νC_2N_3 (5_D); νN_1C_2 (5_B)
		1551 (0)	νC_2N_{12} (16_A); νC_2N_{12} (8_D); νC_2N_{12} (7_B); νC_2N_3 (5_A)
1536 m (2)	1537 w	1546 (1)	νC_2N_{12} (33_C); νN_7C_5 (15_C); νC_2N_3 (14_C); νN_1C_2 (7_C); νN_1C_2 (6_C)
		1518 (0)	νN_7C_8 (31_C); νC_2N_3 (28_C); νC_4N_9 (12_C); νC_8N_9 (11_C); $\delta C_4C_5N_9$ (6_C)
	1515 vw	1507 (0)	νN_7C_8 (18_A); νC_4N_9 (14_A); νC_8N_9 (11_A); νC_2N_3 (5_A); νC_4C_5 (5_A); νC_2N_{12} (5_A)
		1507 (0)	νN_7C_8 (11_B); νN_7C_8 (13_D); νC_4N_9 (10_D); νC_4N_9 (8_B); νC_8N_9 (7_D); νC_8N_9 (6_B)
		1507 (0)	νN_7C_8 (9_B); νN_7C_8 (9_D); νC_4N_9 (7_B); νC_4N_9 (7_D); νC_8N_9 (7_D); νC_8N_9 (5_B) νN_7C_8 (5_A)
		1479 (0)	δN_9C_8H (18_B); νN_7C_8 (17_B); δN_7C_8H (17_B); νC_4N_9 (17_B); νN_3C_4 (10_B); νN_7C_5 (9_B); νC_5C_6 (5_B)
1479 vw (0)	1476 s	1479 (0)	νN_7C_8 (18_D); δN_9C_8H (17_D); δN_7C_8H (17_D); νC_4N_9 (17_B); νN_3C_4 (10_B); νN_7C_5 (9_B); νC_5C_6 (5_B)
		1478 (0)	νN_7C_8 (18_A); δN_9C_8H (17_A); δN_7C_8H (17_A); νC_4N_9 (16_A); νN_3C_4 (9_A); νC_8N_9 (5_A) νC_5C_6 (5_A)
		1478 (0)	νC_4N_9 (20_C); νN_7C_5 (15_C); δN_9C_8H (14_C); δN_7C_8H (13_C); νC_5C_6 (11_C); νN_7C_5 (10_C); $\delta N_3C_4C_5$ (8_C)

[a] s, vs, m, w, and vw refer to strong, very strong, medium, weak, and very weak bands. Only PED values ≥ 5% are mentioned. The numbers in parentheses give the percent contribution in the normal modes, and their subscripts refer to guanosine monomers A, B, C, and D, which are the constituents of the centrosymmetric tetramer (Figure 4). Beside the frequencies, in parentheses, the ^{18}O(6) shifts are defined as $\Delta\nu = \nu(^{16}O) - \nu(^{18}O)$, where $\nu(^{16}O)$ and $\nu(^{18}O)$ are the wavelengths (in reciprocal centimeters) for the normal tetramer and the ^{18}(O)-substituted analogue, respectively.

TABLE 4: Eigenvector Main Components for the νC═O Modes of Guanosine Tetramer

infrared	Raman	calculated	eigenvector main components[a]
	1702 w	1700	νC═O (-0.17_A); νC═O (-0.17_B); νC═O (-0.17_C); νC═O (-0.17_D)
1679 vs		1680	νC═O (0.24_A); νC═O (0.03_B); νC═O (-0.23_C); νC═O (0.03_D); νC_5C_6 (-0.15_A); νC_5C_6(0.16_C)
1670 vs		1673	νC═O (-0.24_B); νC═O(0.24_D); νC_5C_6 (0.15_B); νC_5C_6 (-0.15_D)
	1659 w	1659	νC═O (0.15_A); νC═O (-0.16_B); νC═O (0.14_C); νC═O (-0.16_D); νC_5C_6 (-0.11_A) νC_5C_6 (-0.11_C)

[a] Eigenvectors with values ≥ 0.02 appear in eigenvector main components.

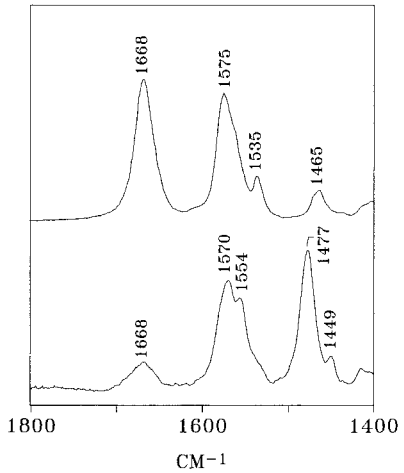

Figure 9. $CDCl_3$ solution infrared (upper) and Raman (lower) spectra of 50 mM N-deuterated silanized guanosine.

not show such a splitting (Figure 9), despite the presence of both hydrogen-bonded and free carbonyl groups in this homodimer (Figure 1).

That the G*G dimer is predominant in the solution of Figure 9 is proven through a simple calculation taking into account the self-association constant of silanized guanosine,[36] which shows that more than 90% of silanized guanosine is present as the dimer. The infrared and Raman νC═O bands of this solution show their maximum intensities at 1668 cm^{-1}, which can be attributed to the free C═O group in the dimer. This νC═O band component masks that of the hydrogen carbonyl group, which is located at the slope of the 1668 cm^{-1} band toward smaller frequencies. The absence of the above splitting of about 20 cm^{-1} in reverse Hoogsteen hydrogen-bonded guanine (Figure 9) can be due to the great distance (6.34 Å) between both carbonyl groups,[13] which does not produces a significant transition moment coupling. Thus, if we use the structure proposed by Thewalt et al.[13] which a C···C distance of 6.34 Å, then we find that for $(\delta\mu/\delta r_{C=O}) = 9$, $f(\nu$C═O, νC═O) is 0.03 mdyn/Å. If we include this intermolelcular interaction force constant in the force field, we obtain a C═O splitting of about 1 cm^{-1}.

In conclusion, we have prepared for the first time ^{18}O(6)-guanosine by enzymatic dechlorination of Cl(6)-guanosine. The enzyme adenylic acid deaminase and the substrate are inexpensive and available commercially, and they can be used for large-scale preparation of this guanosine isotopic derivative. Observations of the vibrational spectra of both guanosine and

^{18}O(6)-guanosine have allowed us to assign the C═O stretching bands of guanosine tetramer, whose infrared and Raman spectra are consistent with a centrosymmetric tetrameric structure belonging to the C_{2h} symmetry point group. The computations of vibrational frequencies show that no normal mode is associated with a single C═O group vibration; the νC═O vibrations are mixed motions of C═O groups. A force field incorporating the transition dipole−dipole coupling for adjacent C═O groups is able to explain the νC═O splittings in guanosine tetramer. As this coupling is inherent in the Hoogsteen structure of hydrogen-bonded guanine nucleobases, νC═O splitting is a characteristic of this structure, unlike the νC═O spectral profile of the reverse Hoogsteen structure, where this splitting is absent. The interest of the spectroscopic characterization of these structures lies in their identification when they are present in G*G·C triplets of nucleic acid triple helices.

Acknowledgment. We are grateful to the Dirección General de Investigación Científica y Técnica (DGICYT) for financial support (Project PB93-0131).

References and Notes

(1) Delabar, J. M.; Guschlbauer, W. M. *Biopolymers* **1979**, *18*, 2073.
(2) Chinsky, L.; Jollès, B.; Laigle, A.; Turpin, P. Y. *J. Raman Spectrosc.* **1987**, *18*, 195.
(3) Leicknam, J. P.; Chauvelier, C.; Chantot, J. F.; Guschlbauer, W. *Biophys. Chem*. **1973**, *1*, 134.
(4) Nishimura, Y.; Tsuboi, M.; Lubasek, W. L.; Bajdor, K.; Peticolas, W. *J. Raman Spectrosc*. **1987**, *18*, 221.
(5) Majoube, M.; Millié, Ph.; Lagant, P.; Vergotten, G. *J. Raman Spectrosc*. **1994**, *25*, 821.
(6) Ouali, M.; Letellier, R.; Sun, J. S.; Akhebat, A.; Adnet, F.; Liquier, J.; Taillandier, E. *J. Am. Chem. Soc*. **1993**, *115*, 4264.
(7) Dagneaux, C.; Porumb, H.; Letellier, R.; Malvy, C.; Taillandier, E. *J. Mol. Struct*. **1995**, *347*, 343.
(8) Williams, N. G.; Williams, L. D.; Shaw, B. R. *J. Am. Chem. Soc*. **1989**, *111*, 7205.
(9) Tougard, P.; Chantot, J.-F.; Guschlbauer, W. *Biochim. Biophys. Acta* **1973**, *308*, 9.
(10) Carmona, P.; Molina, M.; Lasagabaster, A.; Escobar, R. *Biospectroscopy* **1995**, *1*, 235.
(11) Carmona, P.; Lasagabaster, A.; Molina, M. *Biochim. Biophys. Acta* **1995**, *1246*, 128.
(12) Wilson, E. B.; Decius, J. C.; Cross, P. C. *Molecular Vibrations*; McGraw-Hill: New York, 1955.
(13) Thewalt, U.; Bugg, C. E.; Marsh, R. E. *Acta Crystallogr*. **1970**, *B26*, 1089.
(14) Davies, D. R.; Zimmerman, S. B.; Cohen, G. H. *J. Mol. Biol*. **1975**, *92*, 181.
(15) Majoube, M. *J. Chim. Phys*. **1984**, *81*, 303.
(16) Majoube, M. *Biopolymers* **1985**, *24*, 1075.
(17) Bandekar, J.; Zundel, G. *Spectrochim. Acta* **1983**, *39A*, 343.
(18) Moore, W. H.; Krimm, S. *Proc. Natl. Acad. Sci. U.S.A.* **1975**, *72*, 4933.
(19) Wilson, D. K.; Rudolph, F. B.; Quiocho, F. A. *Science* **1991**, *252*, 1278.
(20) Margolin, A. L.; Borcherding, D. R.; Wolf-Kugel, D.; Margolin, N. *J. Org. Chem*. **1994**, *59*, 7214.
(21) Bang, Y. *Biochem. Z*. **1910**, *26*, 293.
(22) Gellert, M.; Lipsett, M. N.; Davies, D. R. *Proc. Natl. Acad. Sci. U.S.A.* **1962**, *48*, 2013.
(23) Chantot, J. F.; Sarocchi, M. T.; Guschlbauer, W. *Biochimie* **1971**, *53*, 347.
(24) Chantot, J. F.; Guschlbauer, W. *FEBS Lett.* **1969**, *4*, 173.
(25) Guschlbauer, W.; Chantot, J. F.; Sarocchi, M. T., Thiele, D. *Stud. Biophys*. **1970**, *24/25*, 29.
(26) Chantot, J. F. *Arch. Biochem. Biophys*. **1972**, *153*, 347.
(27) Lane, M. J.; Thomas, G. J., Jr. *Biochemistry* **1979**, *18*, 3839.
(28) Duguid, J. G.; Bloomfield, V. A.; Benevides, J. M.; Thomas, G. J., Jr. *Biophys. J*. **1995**, *69*, 2623.
(29) Duguid, J. G.; Bloomfield, V. A.; Benevides, J.; Thomas, G. J.; Jr. *Biophys. J*. **1993**, *65*, 1916.
(30) Langlais, M.; Tajmir-Riahi, H. A.; Savoie, R. *Biopolymers* **1990**, *30*, 743.
(31) Tsuboi, M.; Shuto, K.; Higuchi, S. *Bull. Chem. Soc. Jpn*. **1968**, *41*, 1821.
(32) Nishimura, Y.; Tsuboi, M.; Kubasek, W. L.; Bajdor, K.; Peticolas, W. L. *J. Raman Spectrosc*. **1987**, *18*, 221.
(33) Segal, G. A.; Klein, M. L. *J. Chem. Phys*. **1967**, *47*, 4236.
(34) Radziemski, L. J.; Solarz, R. W.; Paisner, J. A. *Laser Spectroscopy and its Applications*; Marcel Dekker: New York, 1987.
(35) Williams, N. G.; Williams, L. D.; Shaw, B. R. *J. Am. Chem. Soc*. **1989**, *111*, 7205.
(36) Carmona, P.; Molina, M.; Lasagabaster, A.; Escobar, R.; Ben Altabef, A. *J. Phys. Chem*. **1993**, *97*, 9519.